Electron Transfer from Heme b_L to the [3Fe-4S] Cluster of *Escherichia coli* Nitrate Reductase A (NarGHI)†

Richard A. Rothery,‡ Francis Blasco,§ and Joel H. Weiner*,‡

CIHR Group in the Molecular Biology of Membrane Proteins, Department of Biochemistry, 474 Medical Sciences Building, University of Alberta, Edmonton, Alberta T6G 2H7, Canada, and Laboratoire de Chimie Bactérienne, CNRS, 31 chemin Joseph Aiguier, 13402 Marseille Cedex 9, France

Received October 16, 2000

ABSTRACT: We have investigated the functional relationship between three of the prosthetic groups of *Escherichia coli* nitrate reductase A (NarGHI): the two hemes of the membrane anchor subunit (NarI) and the [3Fe-4S] cluster of the electron-transfer subunit (NarH). In two site-directed mutants (NarGHI^{H56R} and NarGHI^{H205Y}) that lack the highest potential heme of NarI (heme b_H), a large negative $\Delta E_{m,7}$ is elicited on the NarH [3Fe-4S] cluster, suggesting a close juxtaposition of these two centers in the holoenzyme. In a mutant retaining heme b_H, but lacking heme b_L (NarGHI^{H66Y}), there is no effect on the NarH [3Fe-4S] cluster redox properties. These results suggest a role for heme b_H in electron transfer to the [3Fe-4S] cluster. Studies of the pH dependence of the [3Fe-4S] cluster, heme b_H, and heme b_L E_m values suggest that significant deprotonation is only observed during oxidation of the latter heme (a pH dependence of -36 mV pH^{-1}). In NarI expressed in the absence of NarGH [NarI(ΔGH)], apparent exposure of heme b_H to the aqueous milieu results in both it and heme b_L having E_m values with pH dependencies of approximately -30 mV pH^{-1}. These results are consistent with heme b_H being isolated from the aqueous milieu and pH effects in the holoenzyme. Optical spectroscopy indicates that inhibitors such as HOQNO and stigmatellin bind and inhibit oxidation of heme b_L but do not inhibit oxidation of heme b_H. Fluorescence quench titrations indicate that HOQNO binds with higher affinity to the reduced form of NarGHI than to the oxidized form. Overall, the data support the following model for electron transfer through the NarI region of NarGHI: Q_P site → heme b_L → heme b_H → [3Fe-4S] cluster.

Escherichia coli, when grown anaerobically with nitrate as respiratory oxidant, develops a respiratory chain terminated by a membrane-bound quinol:nitrate oxidoreductase (NarGHI)[1] (*1*, *2*) that can be overexpressed to high levels in the cytoplasmic membrane (*3*−*5*). Intensive biophysical and biochemical characterizations have revealed that NarGHI comprises a molybdenum cofactor-containing [molybdobis-(molybdopterin guanine dinucleotide), Mo-bisMGD] catalytic subunit [(NarG; 139 kDa (*4*)], an [Fe-S] cluster-containing electron-transfer subunit [NarH; 58kDa (*6*)], and a heme-containing membrane-anchor subunit [NarI; 26kDa (*5*)]. The catalytic and electron-transfer subunits comprise a cytoplasmically localized membrane-extrinsic catalytic dimer (NarGH) anchored to the membrane by NarI. The Mo of the nitrate-reducing Mo-bisMGD cofactor has $E_{m,8}$ values of approximately +95 mV [Mo(IV/V)] and +195 mV [Mo(V/VI)] (*3*, *4*, *7*). The NarH [Fe-S] clusters comprise one [3Fe-4S] cluster and three [4Fe-4S] clusters (*6*−*9*). In membranes enriched in NarGHI, the [3Fe-4S] cluster appears to exist as two potentiometrically distinct subpopulations with very similar EPR spectra: a major (70%) component with an $E_{m,8}$ of +180 mV and a minor (30%) component with an $E_{m,8}$ of +100 mV (*3*). The three [4Fe-4S] clusters have $E_{m,8}$ values of +130 mV, −55 mV, and −400 mV (*3*). NarI contains two hemes with $E_{m,7}$ values of +20 mV (heme b_L) and +125 mV (heme b_H) (*10*). Thus, electron transfer through NarGHI potentially involves seven prosthetic groups with E_m values over a range of approximately 600 mV. The precise electron-transfer pathway through the enzyme has yet to be resolved.

The membrane anchor and diheme cytochrome *b* subunit (NarI) is a 225 amino acid protein with five transmembrane helices (TM1−TM5) in which, based on hydropathy analyses and biophysical studies, the N-terminus is periplasmically localized (*5*, *10*, *11*). Both hemes have highly anisotropic low-spin (HALS) EPR spectra (*12*) that are consistent with a near-perpendicular orientation of the imidazole planes of the heme iron ligands (*13*). Heme b_L has a g_z of 3.36, and heme b_H has a g_z of 3.76 (*5*, *10*). Analyses of site-directed

† This work was funded by the Canadian Institutes of Health Research, the Centre National de la Recherche Scientifique, and the Human Frontier Science Program Organization. F.B. was supported by a Visiting Scientist award from the Alberta Heritage Foundation for Medical Research.

* To whom correspondence should be addressed. Tel: (780) 492-2761. Fax: (780) 492-0886.

‡ University of Alberta.

§ Laboratoire de Chimie Bactérienne, CNRS.

[1] Abbreviations: FrdABCD, *Escherichia coli* fumarate reductase; FrdCAB, *Wolinella succinogenes* fumarate reductase; HALS, highly anisotropic low spin; HOQNO, 2-*n*-heptyl-4-hydroxyquinoline *N*-oxide; IPTG, isopropyl 1-thio-β-D-galactopyranoside; Mo-bisMGD, molybdo-bis(molybdopterin guanine dinucleotide); NarGHI, nitrate reductase holoenzyme; NarGH, nitrate reductase soluble dimer; NarI(ΔGH), nitrate reductase cytochrome *b* subunit in the absence of NarGH; PB, 5-hydroxy-2-methyl-1,4-naphthoquinone; PBH_2, reduced PB; SdhCAB, *Bacillus subtilis* succinate dehydrogenase.

10.1021/bi002393k CCC: $20.00
Published on Web 04/05/2001

mutants of NarGHI place heme b_L toward the periplasmic side of NarI (coordinated by His-66 and His-187) and heme b_H toward the cytoplasmic side (coordinated by His-56 and His-205) (*14*). The hemes are coordinated between two transmembrane helices (TM2 and TM5) rather than the four helices found in some other bacterial hydrophobic diheme cytochromes *b* (*15*−*17*). Heme b_H has been localized to the NarGH−NarI interface region on the basis of its modified EPR and redox properties when expressed in the absence of NarGH (*10*). This form of NarI is referred to as NarI(ΔGH), and the modification of the properties of its heme b_H is likely a result of exposure of this center to the aqueous milieu. Also, EPR and potentiometric studies of the purified NarGH dimer indicate that the [3Fe-4S] cluster is modified in the absence of NarI (*7*). In membrane-bound NarGHI the [3Fe-4S] cluster has an $E_{m,8}$ of +180 mV (major component) (*3*), whereas it has an $E_{m,8.3}$ of +60 mV in purified NarGH (*7*). This large negative ΔE_m could also be explained by exposure of the cluster to the aqueous milieu. Thus, both heme b_H and the [3Fe-4S] cluster can tentatively be localized to the NarGH−NarI interface region of the holoenzyme.

Another measure of solvent accessibility that is relevant to the electron-transfer pathway out of NarI is the response of the redox chemistry of the hemes and [3Fe-4S] cluster to variations of pH. The ambient pH can be expected to have a significant effect on the E_m values of centers that are exposed to the aqueous milieu, provided that there are suitable protonatable side chains in the vicinity of the affected center (*18*−*21*). For example, heme edge exposure of heme b_L (due to its probable proximity to the periplasmic side of NarI) might result in the redox chemistry of this heme having a greater pH dependence than that of heme b_H (assuming that the latter is almost completely buried within NarGHI). pH dependence may also be mediated by the residues lining Q-sites or by bound quinone/quinol deprotonations. It would therefore be of interest to determine the pH dependence of the hemes and [3Fe-4S] cluster of NarGHI and the hemes of NarI(Δ*G*H).

The use of the quinol binding site (Q-site) inhibitors HOQNO (2-*n*-heptyl-4-hydroxyquinoline *N*-oxide) and stigmatellin has indicated the presence of a dissociable Q-site in the vicinity of heme b_L toward the periplasmic side of NarI (*10*, *22*). This is consistent with the proposed bioenergetics of NarGHI (*11*, *23*) in which quinol oxidation occurs at a single periplasmically oriented dissociable Q-site, releasing protons into the periplasm during enzyme turnover. However, three lines of evidence suggest the presence of an additional Q-site (the Q_{nr}-site) that is located within the NarGH dimer. (i) A single menaquinone-9 molecule copurifies with the NarGH dimer (*24*). (ii) Both HOQNO and stigmatellin appear to inhibit nitrate-dependent heme oxidation (*22*). (iii) Two apparent sites of quinol binding were detected in one analysis of the steady-state kinetics of quinol oxidation (*25*). However, in two other studies kinetics were observed that are consistent with quinol binding and oxidation occurring at a single site (the Q_P-site) (*26*, *27*). Thus, further clarification is necessary of the relationships between the Q-site(s) and the prosthetic groups of the membrane-intrinsic arm of the electron-transfer conduit through NarGHI.

In this paper, we have studied the relationship between heme b_H of NarI and the [3Fe-4S] cluster of NarH by redox potentiometry in combination with EPR spectroscopy. We have investigated the solvent exposure of the [3Fe-4S] cluster and the two hemes of NarGHI and the two hemes of NarI(ΔGH) by performing redox titrations at a range of pH values. In addition, we have reinvestigated the phenomenon of HOQNO- and stigmatellin-dependent inhibition of heme oxidation and have determined the effect of the redox state of the protein on its affinity for HOQNO. In the absence of detailed structural data, these studies provide important information on the electron-transfer pathway from the dissociable Q_P site of NarI to the [3Fe-4S] cluster of NarH.

MATERIALS AND METHODS

Bacterial Strains and Plasmids. E. coli LCB2048 [*thi-1*, *thr-1*, *leu-6*, *lacY1*, *supE44*, *rpsL175* Δnar25(*narG-narH*) Δ(*nar′U-narZ′*), Ω (Spc^R), Km^R] (*28*) was used as the host for all the experiments described herein. Wild-type, NarI-H56R, NarI-H66Y mutant NarGHI were expressed from pVA700, pVA700-H56R, and pVA700-H66Y, respectively (*5*). NarI-H205Y mutant enzyme was expressed from pVA700-H205Y which was constructed as previously described (*5*). NarI(ΔGH) was expressed from plasmid pCD7 (*5*). pVA700 and pCD7 bear their respective genes under the control of the *tac* promoter.

Growth of Cells and Preparation of Membrane Vesicles Enriched in Wild-Type and Mutant NarGHI. Cells were grown microaerobically overnight in 2 L batch cultures of Terrific Broth (*29*) at 30 °C in the presence of 100 μg mL^{-1} streptomycin, 100 μg mL^{-1} ampicillin, and 50 μg mL^{-1} kanamycin as previously described (*10*). Protein overexpression was induced by addition of 0.2 mM isopropyl 1-thio-β-D-galactopyranoside (IPTG) to the growth cultures. Crude membranes were prepared by French pressure cell lysis and differential centrifugation in 100 mM MOPS and 5 mM EDTA (pH 7.0) which contained the protease inhibitor phenylmethanesulfonyl fluoride (0.2 mM) (*30*). Cytoplasmic membranes were isolated from resuspended crude membranes by layering them on top of a 55% (w/v) sucrose step (made up in buffer) in an ultracentrifuge tube. Following centrifugation at 40 000 rpm for 2 h, the floating band enriched in the cytoplasmic membrane fraction was removed, diluted in buffer, and subjected to a further centrifugation. Finally, to ensure complete removal of residual sucrose, the pellet was resuspended in buffer and recentrifuged. Membranes were then resuspended in buffer to a protein concentration of approximately 30 mg mL^{-1}, flash frozen in liquid nitrogen, and stored at −70 °C until use. Membranes of LCB2048 lacking NarGHI were prepared as described above except that ampicillin and IPTG were omitted from the growth medium.

Growth of Cells and Preparation of Membrane Vesicles Enriched in NarI(ΔGH). Cells (LCB2048/pCD7) were grown as described above, except that the growth temperature was 37 °C and the cultures were grown for 4 h rather than overnight. The cytoplasmic membrane fraction was isolated as described above.

Redox Potentiometry and EPR Spectroscopy. Redox titrations were carried out under argon at 25 °C as previously described (*31*) in the following buffers, each of which also contained 5 mM EDTA: 100 mM MES (pH 5.5 and 5.9); 100 mM MOPS (pH 6.7); 100 mM HEPES (pH 7.5); 100

mM Tricine (pH 8.0 and 8.5), and 100 mM CHES (pH 9.0). Prior to carrying out the titrations, membranes were thawed, diluted in the appropriate buffer, pelleted by ultracentrifugation, and resuspended in buffer to a protein concentration of approximately 30 mg mL^{-1}. The following redox mediators were used at a concentration of 50 μM: quinhydrone, 2,6-dichloroindophenol, 1,2-naphthoquinone, toluylene blue, phenazine methosulfate, thionine, duroquinone, methylene blue, resorufin, indigotrisulfonate, indigodisulfonate, anthraquinone-2-sulfonic acid, phenosafranine, benzyl viologen, and methyl viologen. All samples were prepared in 3 mm internal diameter quartz EPR tubes and were rapidly frozen in liquid nitrogen chilled ethanol and stored under liquid nitrogen until use. EPR spectra were recorded using a Bruker ESP300 spectrometer equipped with an Oxford Instruments ESR-900 flowing helium cryostat. [3Fe-4S] cluster E_m values were obtained from plots of signal intensity of the $g = 2.02$ peak in spectra of potentiometrically poised samples versus E_h in spectra recorded under the EPR conditions described in the legend to Figure 1. Heme E_m values were obtained from spectra recorded at 12 K with a modulation amplitude of 20 G_{pp}. For analyses of heme b_H ($g_z = 3.76$), spectra were recorded at a microwave power of 100 mW, whereas for heme b_L ($g_z = 3.36$) spectra were recorded at a microwave power of 20 mW. In all cases, estimates of E_m were obtained from $n = 1$ fits of the potentiometric data to the Nernst equation. Where appropriate, EPR spin quantitations were carried out as previously described (*32*) using a 1 mM CuEDTA sample as standard.

Optical Spectroscopy. Kinetic data on the quinol-dependent reduction and nitrate-dependent oxidation of the hemes of NarGHI were collected using a Hewlett-Packard 8453 diode array spectrophotometer equipped with a Hewlett-Packard 89090A Peltier temperature controller/cuvette stirrer. All experiments were carried out at 23 °C. Experiments were carried out in N_2-saturated 100 mM MOPS, 5 mM EDTA, and 20 mM glucose (pH 7.0) using 4 mL acryl cuvettes (Sarstedt 67.738) with machined Teflon stoppers constructed in the Faculty of Medicine's Biomedical Workshop (University of Alberta) (*27*). These had a 11 mm plug that inserted into the acryl cuvettes, creating an effective seal against oxygen diffusion. As an additional precaution against residual oxygen diffusion into the cuvettes, 5 units of glucose oxidase containing trace amounts of catalase (Sigma G-6891) were added to each cuvette prior to each experiment (*33*). Each cuvette was stirred using a spinbar (37150 Cell Spinbar) rotating at 200 rpm. Quinones (plumbagin or lapachol) were reduced by zinc in acidified ethanol (*27*). Additional details of the optical experiments performed are described in the legend to Figure 4.

Fluorescence Quench Titrations. The affinity of NarGHI and NarI(ΔGH) for HOQNO was determined using fluorescence quench titrations performed as previously described using a Perkin-Elmer LS-50B luminescence spectrometer (*10*, *34*) with the following modifications. Experiments were carried out in acryl fluorescence cuvettes (Sarstedt 67.755) with machined Teflon stoppers similar to those described above. N_2-saturated 100 mM MOPS and 5 mM EDTA (pH 7.0) were added to the cuvette, and fluorescence quench titrations were carried out in the presence of oxidized or reduced duroquinone (reduced as described above).

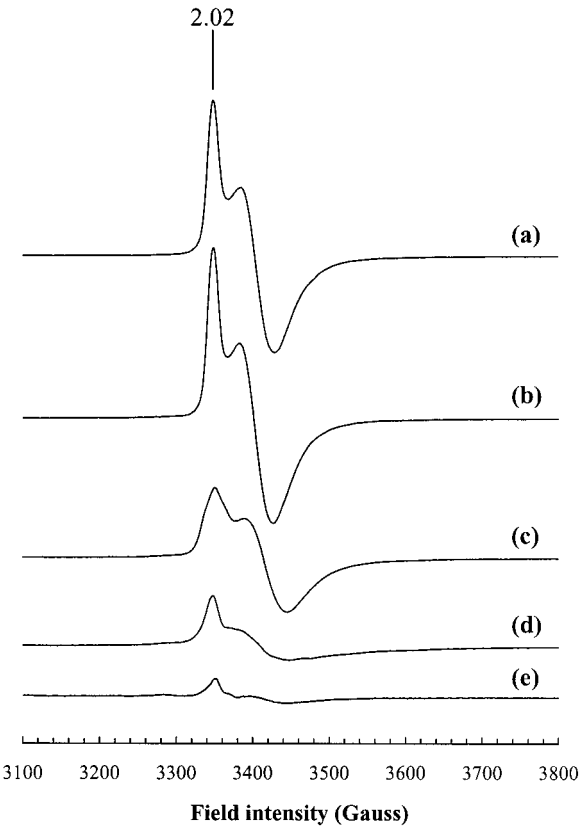

FIGURE 1: Effect of heme b_H mutants on the [3Fe-4S] cluster EPR spectrum. EPR spectra were recorded of inner membrane samples of strains overexpressing wild-type and mutant NarGHI. Spectra: (a) wild-type; (b) $NarGHI^{H66Y}$; (c) $NarGHI^{H205Y}$; (d) $NarGHI^{H56R}$; (e) background strain (LCB2048). EPR conditions: temperature, 12 K; microwave power, 20 mW at 9.47 GHz; modulation amplitude, 10 G_{pp} at 100 kHz. Samples were oxidized with an excess of dichloroindophenol (a−d) or ferricyanide (e). The vertical line represents a *g*-value of 2.02.

Protein Assays. Protein concentrations were assayed by the Lowry method, modified by the inclusion of 1% (w/v) sodium dodecyl sulfate in the incubation mixture to solubilize membrane proteins (*35*).

RESULTS

Effect of the Loss of Heme b_H on the EPR Spectrum of the [3Fe-4S] Cluster of NarGHI. On the basis of optical and EPR spectroscopy, $NarGHI^{H56R}$ and $NarGHI^{H205Y}$ both lack heme b_H, whereas $NarGHI^{H66Y}$ lacks heme b_L (*5*, *14*). Thus, these mutants enabled us to investigate the effect of the absence of either of the hemes on the EPR spectrum of the NarH [3Fe-4S] cluster. Figure 1 shows EPR spectra of oxidized membranes containing no NarGHI (membranes from untransformed *E. coli* LCB2048, Figure 1e) and membranes enriched in NarGHI (Figure 1a), $NarGHI^{H66Y}$ (Figure 1b), $NarGHI^{H205Y}$ (Figure 1c), and $NarGHI^{H56R}$ (Figure 1d). EPR spectra of oxidized wild-type NarGHI and $NarGHI^{H66Y}$ in membranes are identical to those previously reported by us (*3*, *5*, *10*) and indicate that the environment of the [3Fe-4S] cluster is unaltered in the NarI-H66Y mutant. In contrast, the spectra of $NarGHI^{H205Y}$ (Figure 1c) and $NarGHI^{H56R}$ (Figure 1d) are significantly altered compared to the wild type. In $NarGHI^{H205Y}$, the signal appears broader, and in the case of $NarGHI^{H56R}$, there is a significant diminution of intensity compared to the wild type. Spin

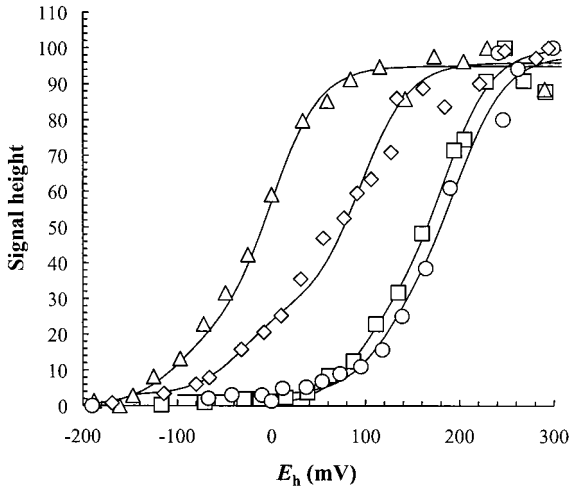

FIGURE 2: Effect of heme b_H mutants on the midpoint potential of the NarH [3Fe-4S] cluster. Data were obtained from EPR spectra recorded under the conditions described for Figure 1. Symbols: squares, NarGHI [$E_{m,7}$ values: +185 mV (70%); +100 mV (30%)]; circles, NarGHI^{H66Y} [$E_{m,7}$ values: +200 mV (68%); +125 mV (32%)]; diamonds, NarGHI^{H205Y} [$E_{m,7}$ values: +95 mV (73%); −30 mV (27%)]; triangles, NarGHI^{H56R} [$E_{m,7}$ values: 0 mV (78%); −90 mV (22%)]. For each titration presented, data were normalized to a maximum intensity of 100.

quantitation of the samples used to generate the spectra of Figure 1 indicates that they contained 1.68, 1.86, 1.52, 1.15, and 0.31 nmol (mg of protein)$^{-1}$ detectable [3Fe-4S] cluster in membranes containing wild-type NarGHI, NarGHI^{H66Y}, NarGHI^{H205Y}, NarGHI^{H56R} and membranes containing no NarGHI, respectively, in reasonable agreement with previously reported values (*10*).

Redox Potentiometry of the [3Fe-4S] Cluster in NarGHI, NarGHI^{H66Y}, NarGHI^{H205Y}, and NarGHI^{H56R}. In the recently determined structure of *Wolinella succinogenes* fumarate reductase (FrdCAB), one of the hemes (heme b_P) of the membrane anchor subunit (FrdC) is located approximately 11 Å from the [3Fe-4S] cluster that is located in FrdB (*17*). This, and our previous observations that heme b_H of NarI(ΔGH) has a significantly altered EPR spectrum and modified electrochemistry compared to what is found in NarGHI (*10*), prompted us to investigate the effect of the loss of heme b_H on the electrochemistry of the [3Fe-4S] cluster of NarGHI. Figure 2 shows potentiometric titrations of the [3Fe-4S] cluster in NarGHI, NarGHI^{H66Y}, NarGHI^{H205Y}, and NarGHI^{H56R}. In the wild-type enzyme, the [3Fe-4S] cluster titrates with a major $E_{m,7}$ of +185 mV (70%) and a minor $E_{m,7}$ of +100 mV (30%), in close agreement with previously published values (*3*, *10*). In the case of NarGHI^{H66Y}, which lacks heme b_L but retains heme b_H, the [3Fe-4S] cluster titrates with a major $E_{m,7}$ of +200 mV (68%) and a minor $E_{m,7}$ of +125 mV (32%), indicating that loss of heme b_L has little effect on the redox chemistry of the [3Fe-4S] cluster. In contrast, mutants in which heme b_H is absent have significantly modified [3Fe-4S] cluster redox chemistry: in NarGHI^{H205Y} the [3Fe-4S] cluster titrates with a major $E_{m,7}$ of +95 mV (73%) and a minor $E_{m,7}$ of −30 mV (27%); in NarGHI^{H56R} the [3Fe-4S] cluster titrates with a major $E_{m,7}$ of 0 mV (78%) and −90 mV (22%). We also investigated the effect of the heme mutants on the redox chemistry of the highest potential [4Fe-4S] cluster (by analyzing plots of the intensity of the $g = 1.87$ peak−trough [4Fe-4S] cluster EPR feature versus E_h; data not shown). The highest potential [4Fe-4S] cluster has an $E_{m,7}$ of approximately 125, 120, 110, and 110 mV in membranes containing wild-type, NarI-H66Y, NarI-H205Y, and NarI-H56R, respectively. These data are summarized in Table 1 and indicate that the absence of heme b_H in the NarI-H205Y and NarI-H56R mutants modifies the environment of the [3Fe-4S] cluster, yet has little effect on the highest potential [4Fe-4S] cluster.

Table 1: Effect of Heme Ligand Mutants on [3Fe-4S] Cluster E_m Values

	[3Fe-4S] cluster			highest potential [4Fe-4S] cluster
mutant (ligand to)	E_m-H (%) (mV)	E_m-L (%) (mV)	$\Delta E_{m,7}$-H[a] (mV)	E_m (mV)
wild type	185 (70%)	100 (30%)		125
NarI-H56R (b_H)	0 (78%)	−90 (22%)	−185	110
NarI-H205Y (b_H)	95 (73%)	−30 (27%)	−90	110
NarI-H66Y (b_L)	200 (68%)	125 (32%)	+15	120

[a] Change in $E_{m,7}$ elicited on the major subpopulation of the [3Fe-4S] cluster compared to the wild-type enzyme.

pH Dependencies of the [3Fe-4S] Cluster, Heme b_H, and Heme b_L Midpoint Potentials. The pH dependence of the E_m values can provide important information on the involvement of redox-coupled protonations in enzyme turnover (*18*, *19*, *21*). Redox titrations of the NarGHI [3Fe-4S] cluster performed at pH 5.9 and 8.5 indicate that the major components titrate with E_m values of +195 and +170 mV, respectively (data not shown). Similar titrations performed on the hemes of NarGHI with data generated from the intensities of the $g = 3.76$ peak (heme b_H) and the $g = 3.36$ peak (heme b_L) at pH 5.9 and 8.5 indicate that heme b_H titrates with E_m values of +110 and +90 mV, respectively. In contrast to the relatively low apparent pH dependence of the E_m of both the [3Fe-4S] cluster and heme b_H, heme b_L titrates with E_m values of +30 and −60 mV at pH 5.9 and 8.5, respectively, indicating a much more significant apparent dependence on pH than for the other two prosthetic groups studied herein. To further investigate the effect of pH on the E_m values of the [3Fe-4S] cluster and the two hemes, we carried out redox titrations at a number of pH values between 5.5 and 9.0 (Figure 3a). It is clear that the two [3Fe-4S] cluster components and heme b_H both have a relatively low pH dependence of approximately −15 mV pH^{-1}, whereas heme b_L has a pH dependence of −36 mV pH^{-1} (Table 2). The data clearly indicate that heme b_L appears to be more susceptible to the pH of the aqueous milieu than either heme b_H or the [3Fe-4S] cluster.

In the absence of the NarGH dimer in NarI(ΔGH), we have shown that the E_m of heme b_H is approximately 300 mV lower than it is in the NarGHI holoenzyme (*10*). Likewise, the apparent E_m of the [3Fe-4S] cluster has been determined to be approximately 120 mV lower in the NarGH dimer compared to its value in NarGHI (*7*, *10*). Both of these observations can be interpreted in terms of increased exposure of the prosthetic group to the aqueous milieu, resulting in a significant $-\Delta E_m$. To further explore this possibility in the case of heme b_H, we investigated the effect of pH on the E_m values of both hemes in NarI(ΔGH) (Figure 3b). In this case, both hemes exhibit a pH dependence of approximately −30 mV pH^{-1} (Table 2).

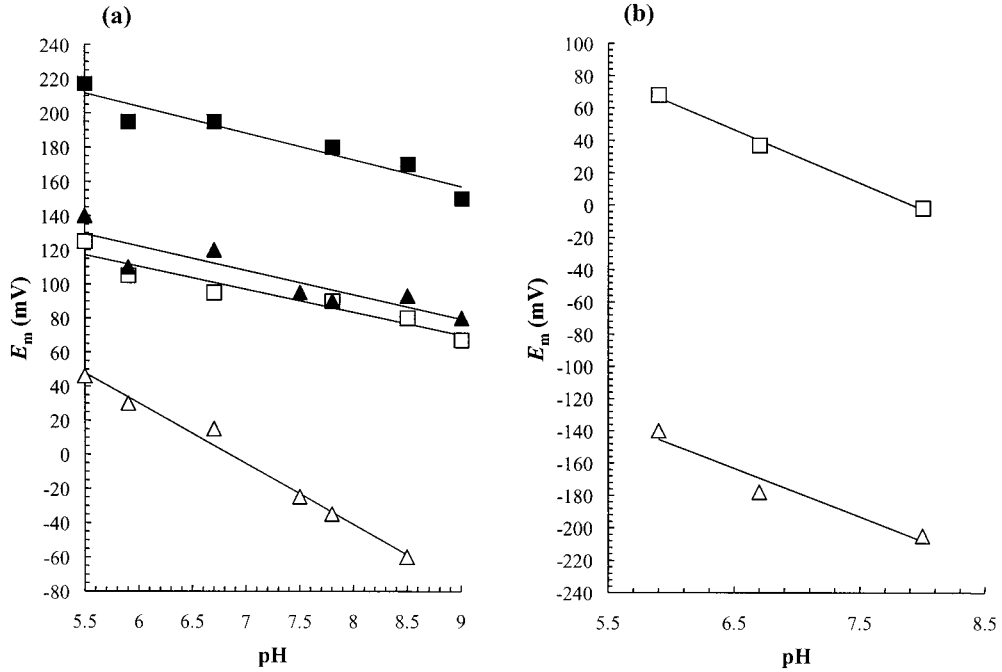

FIGURE 3: (a) Effect of pH on the E_m values of the hemes and [3Fe-4S] cluster of NarGHI. Symbols: closed squares, high-potential [3Fe-4S] cluster component ([3Fe-4S]-H), −16 mV pH^{-1}; open squares, low-potential [3Fe-4S] cluster component ([3Fe-4S]-L), −14 mV pH^{-1}; closed triangles, heme b_H, −14 mV pH^{-1}; open triangles, heme b_L, −36 mV pH^{-1}. Data were obtained from potentiometric redox titrations followed by EPR spectroscopy at 12 K and 20 mW for the [3Fe-4S] clusters ($g = 2.02$ signal), 12 K and 100 mW for the heme b_H signal ($g = 3.76$), and 12 K and 20 mW for the heme b_L signal ($g = 3.36$). (b) Effect of pH on the midpoint potentials of the hemes of NarI(ΔGH). EPR spectra were recorded at 12 K at a microwave power of 2 mW (9.47 GHz) and a modulation amplitude of 20 G_{pp}. Symbols: open squares, heme b_L (−33 mV pH^{-1}); open triangles, heme b_H (−30 mV pH^{-1}).

Table 2: pH Dependence of the NarH [3Fe-4S] Cluster and the Two Hemes of NarI

prosthetic group or subpopulation[a]	$E_{m,7}$[b] (mV)	pH dependence (mV pH^{-1})
[3Fe-4S]-H	188	−16
[3Fe-4S]-L	97	−14
b_H	108 (−178)[c]	−14 (−30)
b_L	−5 (30)	−36 (−33)

[a] The [3Fe-4S] cluster appears as two subpopulations, one of higher ([3Fe-4S]-H) and one of lower ([3Fe-4S]-L) midpoint potential (*3*, *10*). [b] Values at exactly pH 7.0 estimated by interpolation from the fits to the data of Figure 3. [c] Numbers in parentheses indicate the $E_{m,7}$ and their pH dependencies in NarI(ΔGH).

HOQNO-Dependent Inhibition of Heme Reoxidation. It has previously been suggested that there is a second site of inhibitor and quinol binding located between heme b_H and the [3Fe-4S] cluster of NarH (*22*). The data presented above suggest that the arrangement of the NarH [3Fe-4S] cluster and heme b_H is similar to that found in *W. succinogenes* FrdCAB, in which the heme edge is located ∼11 Å from the cluster, with no obvious Q-site in between. However, Magalon et al. (*22*) clearly demonstrated inhibition by HOQNO of nitrate-dependent heme oxidation in an assay system utilizing sodium borohydride-reduced menadione as reductant. Because of the excess reductant often utilized in such assays, we reevaluated the effect of HOQNO on heme oxidation using an assay system in which no excess reductant is present and in which a quinol substrate that has a clearly resolved visible-region absorption peak is used. This assay is based on the use of reduced plumbagin (PBH_2; 5-hydroxy-2-methyl-1,4-naphthoquinol) that has been reduced by zinc in acidified ethanol (*27*).

Traces a and b in Figure 4 show PBH_2-dependent heme reduction and nitrate reoxidation in membranes lacking NarGHI (LCB2048 membranes). PBH_2 elicits heme reduction (Figure 4b) which does not appear to be reoxidized significantly by addition of nitrate. The rate of nitrate-dependent PBH_2 oxidation (Figure 4a) is insignificant compared to that observed in membranes containing overexpressed NarGHI (see below). Traces c and d in Figure 4 show the effect of 54 μM HOQNO on PBH_2-dependent heme reduction and nitrate-dependent heme reoxidation in membranes lacking NarGHI. The only significant change elicited by HOQNO is a slight inhibition of nitrate-dependent PBH_2 oxidation. Figure 4f shows PBH_2-dependent heme reduction and nitrate-dependent heme reoxidation in membranes containing overexpressed NarGHI (LCB2048/pVA700 membranes). In this case, PBH_2 elicits a significant heme reduction (Figure 4f), and subsequent addition of nitrate causes a rapid heme oxidation which is accompanied by a rapid oxidation of the PBH_2 initially added to the cuvette (Figure 4e). Figure 4h shows the effect of 54 μM HOQNO on PBH_2-dependent heme reduction and nitrate-dependent heme reoxidation. Within the time scale of the technique used, no inhibition by HOQNO of PBH_2-dependent heme reduction is observed (Figure 4h). However, the kinetics of nitrate-dependent heme oxidation appear to reflect a mechanism in which approximately 50% of the heme is rapidly oxidized with the remaining heme being oxidized after exhaustion of PBH_2 (Figure 4g). This is supported by the observation that the second step of heme reoxidation is concurrent with complete PBH_2 oxidation. Similar results are obtained when the alternative chromogenic quinol-reduced lapachol is used. Stigmatellin elicits inhibition kinetics similar to those observed with HOQNO (data not shown).

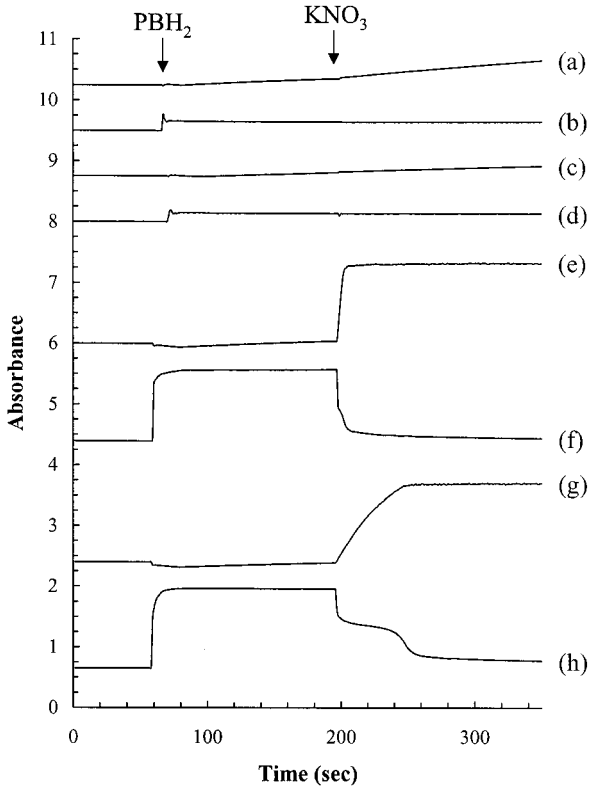

FIGURE 4: Use of reduced plumbagin to follow heme and quinol redox states in the presence of HOQNO. Membranes from a strain lacking NarGHI (a−d) and from a strain overexpressing NarGHI (e−h) at approximately 1 mg mL^{-1} protein were incubated in N_2-saturated 100 mM MOPS/5 mM EDTA/20 mM glucose (pH 7) to which 1.7 units mL^{-1} glucose oxidase had been added. After incubation for at least 60 s, reduced plumbagin (PBH_2) was added to a concentration of 0.35 mM. Following a further 140 s incubation, nitrate (KNO_3) was added to a concentration of 8.7 mM. Where appropriate (traces c, d, g, and h), HOQNO was present at a concentration of 54 μM. $OD_{560-575}$ ($\times$11.25) was used to follow the responses of the hemes present in the membrane samples (traces b, d, f, and h). $OD_{419-575}$ ($\times$1.0) was used to follow the appearance of oxidized plumbagin (PB) (traces a, c, e, and g). HOQNO was present in the experiments represented by traces c, d, g, and h). Absorbance values were offset on the absorbance axis to aid presentation.

Effect of the Heme Reduction State on the Affinity of NarGHI for HOQNO. We have previously demonstrated that both HOQNO and stigmatellin raise the E_m of heme b_L [HOQNO, $\Delta E_m = +100$ mV; stigmatellin, $\Delta E_m = +30$ mV (*10*)]. This is consistent with the heme b_L-associated Q_P site having a greater affinity for HOQNO (and stigmatellin) when the heme is reduced compared to when it is oxidized. This phenomenon could explain the unusual heme reoxidation kinetics in the presence of either of the two inhibitors, and this was tested by measuring the K_d of reduced and oxidized NarGHI for HOQNO by fluorescence quench titration (*10*, *34*). A range of quinol/quinone species were tested: plumbagin, lapachol (*27*), menadione, and duroquinone. Of these, only duroquinone was found to not interfere with the fluorescence of HOQNO under the experimental conditions used herein.

Figure 5 shows fluorescence quench titrations carried out in the presence of duroquinone and duroquinol. In the presence of duroquinone, NarGHI binds HOQNO with a K_d of 0.34 μM (1.3 μM binding sites in a sample containing 0.87 mg mL^{-1} membrane protein). In the presence of duroquinol, the K_d is 0.07 μM (1.3 μM binding sites). Thus, duroquinol-mediated heme reduction significantly increases the affinity of the enzyme for HOQNO.

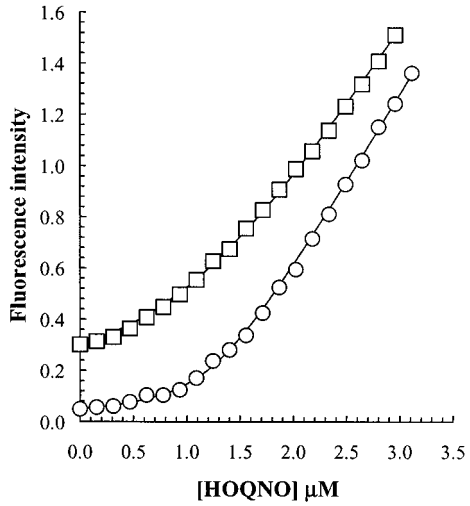

FIGURE 5: Effect of heme redox state on the affinity of NarGHI for HOQNO. Symbols: open squares, membranes incubated in the presence of 0.31 mM oxidized duroquinone; open circles, membranes incubated in the presence of 0.31 mM reduced duroquinone. Data were fit to K_d values for HOQNO of 0.34 μM (oxidized) and 0.07 μM (reduced). In both cases, the concentration of HOQNO binding sites was estimated to be 1.3 μM at a protein concentration of 0.87 mg mL^{-1}.

DISCUSSION

The modification of the EPR spectrum of the NarH [3Fe-4S] cluster in mutants lacking heme b_H but not in the mutant lacking heme b_L is consistent with heme b_H being in close juxtaposition with the [3Fe-4S] cluster in the NarGHI holoenzyme. This is supported by the effect of the mutants on the $E_{m,7}$ of the [3Fe-4S] cluster; mutants of the His ligands to heme b_H elicit a large negative $\Delta E_{m,7}$ on the [3Fe-4S] cluster, whereas the mutant of a His ligand to heme b_L has little or no effect. The increased intensity of the effect in $NarGHI^{H56R}$ compared to $NarGHI^{H205Y}$ may be due to the cluster being closer to NarI-H56 than to NarI-H205. These data suggest that the overall orientation of the heme and [3Fe-4S] cluster may be similar to that observed in the crystal structure of *W. succinogenes* FrdCAB (*17*), with the cluster−heme edge distance being approximately 11 Å. In the structure of *W. succinogenes*, there is no evidence for a Q-site located between the proximal heme of FrdC and the [3Fe-4S] cluster of FrdB, but there is evidence for a Q-site located in the vicinity of the distal heme (*36*). In the structurally closely related succinate dehydrogenase (SdhCAB) from *Bacillus subtilis*, succinate-dependent MQ reduction is eliminated in mutants lacking the distal heme (*37*). Thus, although there is no sequence similarity between NarI and *W. succinogenes*/*B. subtilis* FrdC/SdhC, it is clear that a broadly similar arrangement of Q-sites and hemes exists in both families of proteins: the [3Fe-4S] cluster is in close proximity to the proximal heme (heme b_H in NarI), and quinol binding occurs in the vicinity of the distal heme (heme b_L in NarI). This is despite the fact that the two hemes are coordinated by four TM helices in FrdC/SdhC, but in NarI they are coordinated by two TM helices.

It has previously been suggested that there may be two distinct regions of dissociable quinol binding within NarGHI,

one located in the vicinity of heme b_L (Q_P) and the other located between heme b_H and the [3Fe-4S] cluster (Q_{nr}) (*22*). In some respects, such an arrangement of Q-sites would be similar to that observed in the structure of *E. coli* fumarate reductase (FrdABCD) (*38*). In FrdABCD, menaquinone is observed to bind at a Q_P-site (*P*roximal to the FrdAB dimer) and at a Q_D-site (*D*istal to the FrdAB dimer). It has been demonstrated that HOQNO binding to the FrdABCD Q_P-site perturbs the EPR spectrum of the [3Fe-4S] cluster (*39*, *40*), whereas no such perturbation of the NarH [3Fe-4S] cluster is observed in NarGHI (*10*). This is consistent with there being an HOQNO binding site within approximately 11 Å of the [3Fe-4S] cluster of FrdB [based on the structure of Iverson et al. (*38*)] and there being no such site within an equivalent distance of the [3Fe-4S] cluster of NarH. In NarGHI, the evidence for a heme b_L-associated dissociable Q_P site is compelling (*10*, *22*) and its presence and proposed location toward the periplasmic side of NarI are entirely consistent with the proposed bioenergetics of respiratory nitrate reduction by *E. coli* and other bacteria (*10*, *11*, *23*). The proposed presence of a second Q-site, the Q_{nr}-site, is more problematic. The presence of two dissociable and redox-active Q-sites, one located toward the periplasmic side (the Q_P-site) and one located toward the cytoplasmic side (the Q_{nr}-site) of NarI would generate a conflict with the proposed bioenergetics of NarGHI with the transmembrane proton electrochemical potential rendering a cytoplasmically oriented site more active than a periplasmically oriented site. However, the putative Q_{nr}-site could exist but be nondissociable, such as the nondissociable sites found in *E. coli* cytochrome *bo* (*41*−*43*) and in the well-characterized bacterial photoreaction center (the so-called Q_A site) (*44*, *45*).

Because quinol redox reactions are proton dependent and the possibility that protonatable amino acid side chains may therefore be involved in defining the putative Q_P- and Q_{nr}-sites of NarGHI, we determined the effect of pH on the E_m values of the three prosthetic groups potentially involved in directly accepting electrons from reduced quinols during enzyme turnover. Prosthetic groups that are either directly exposed to the aqueous milieu or undergo redox linked protonation would be expected to have a higher pH dependence than those isolated from these phenomena. Of the three prosthetic groups studied herein, only the E_m of heme b_L has a significant pH dependence (−36 mV pH^{-1}). Given that heme b_H and the [3Fe-4S] cluster both have a dependence of approximately −15 mV pH^{-1}, we are reluctant to interpret the pH dependence of heme b_L in terms of a formal number of protons being taken up upon its reduction. We have previously demonstrated that, in NarI(ΔGH), the $E_{m,7}$ of heme b_H undergoes a $\Delta E_{m,7}$ of approximately −300 mV compared to its value in NarGHI, and this change has been interpreted in terms of exposure of this heme to the aqueous milieu (*10*). In NarI(ΔGH) both hemes have a pH dependence of approximately −30 mV pH^{-1}, suggesting that this effect may also be mediated by heme edge exposure in NarI(ΔGH). The propionate-bearing heme edges are oriented toward the outside edge of the membrane in both the cytochrome *b* subunit of the cytochrome bc_1 complex (*46*) and in the cytochrome *b* subunit (FrdC) of *W. succinogenes* FrdCAB (*17*). In the case of NarI(ΔGH), the absence of NarGH would render the heme b_H propionates more accessible to the aqueous milieu. This is consistent with the observed pH dependence of approximately −30 mV pH^{-1} being mediated by heme propionate exposure to the aqueous milieu. Alternatively, the pH dependence may arise from multiple protonatable groups with weakly coupled pK_a values that are within the pH range studied. Overall, the pH dependence data presented herein support a model for NarGHI in which both the [3Fe-4S] cluster and heme b_H are relatively isolated from pH effects.

The pH dependencies of the heme and [3Fe-4S] cluster E_m values bear interesting comparison with those reported for the two hemes of the cytochrome bc_1 complex and those reported for [Fe-S] clusters in general. In the case of the cytochrome bc_1 complex, hemes b_H and b_L have apparent pH dependencies of approximately −37 and −27 mV, respectively (*47*). These values are in approximate agreement with those reported herein for hemes b_H and b_L of NarI(ΔGH), but only for heme b_L in NarGHI. In the cytochrome bc_1 complex, electrons from quinol oxidation at the Q_o site are transferred both to heme b_L (and then to heme b_H) and to the Rieske [2Fe-2S] cluster (*46*). In contrast to what is observed for the [3Fe-4S] cluster of NarGHI (a pH dependence of approximately −15 mV pH^{-1}), the Rieske cluster exhibits a well-defined pH dependence of approximately −60 mV pH^{-1} above a well-defined pK_a of approximately 7.5 (*18*, *48*). The pH dependence of the E_m of the NarGHI [3Fe-4S] cluster is more typical of that found in a range of [Fe-S] proteins in which no well-defined pK_a is observed (*20*).

The precise origin of the low-potential (minor) component of the [3Fe-4S] cluster signal is not known. It is notable that its E_m and pH dependence are very similar to those of heme b_H. It is therefore tempting to speculate that the low-potential subpopulation of the [3Fe-4S] arises as a result of a redox interaction between the [3Fe-4S] cluster and heme b_H. However, it has also been reported that its potential (and that of the highest potential [4Fe-4S] cluster) is significantly lowered in apomolybdo-NarGHI (*3*) and that there is negative redox cooperativity between these centers in the NarGH dimer (*7*). Thus, further studies will be required to clarify the redox interactions between the [Fe-S] clusters of NarGHI.

The effect of the loss of heme b_H in the NarI-H56R/NarI-H205Y mutants and the pH dependence data are consistent with a model for NarGHI in which there is only a short distance between the [3Fe-4S] cluster and heme b_H. However, it is clear that such a model does not explain the previously reported apparent inhibition of nitrate-dependent heme oxidation (*22*). To resolve this issue, we reduced the hemes of NarGHI with PBH_2 (*27*). By avoiding the use of excessive amounts of reductants such as sodium borohydride, we were able to observe heme reduction that appears to be exclusively quinol-dependent (Figure 4). As previously reported (*22*), there appeared to be little inhibition by HOQNO of PBH_2-dependent heme reduction on the time scale of the experiments reported herein. Addition of nitrate to PBH_2-reduced HOQNO-inhibited membranes elicited a two-step oxidation of the hemes (each phase representing approximately 50% of the total 560−575 nm absorbance), with the second phase being concurrent with the exhaustion of reducing substrate (PBH_2). These observations are consistent with nitrate being able to oxidize heme b_H but not heme b_L in the presence of an excess of quinol and HOQNO.

The observed inhibition by HOQNO of electron transfer between heme b_L and heme b_H is consistent with the Q_P-site having a higher affinity for HOQNO when heme b_L is reduced. This is in agreement with the large positive $\Delta E_{m,7}$ elicited by HOQNO on heme b_L in redox titrations of NarGHI (*10*), potentially explaining the observed inhibition without invoking the presence of a dissociable, inhibitor-binding Q_{nr}-site. To further test this hypothesis, we measured the K_d in the presence of both reduced and oxidized quinol (Figure 5). In the presence of oxidized quinol, the K_d for HOQNO is approximately 0.34 μM, whereas in the presence of reduced quinol it is 0.07 μM. Quinol-dependent heme reduction has no effect on the concentration of HOQNO binding sites. These data are consistent with the following hypothesis for the effect of HOQNO on nitrate-dependent heme oxidation. (i) The rapid first phase is due to oxidation of heme b_H, and its kinetics are defined solely by the rate of nitrate reduction by the Mo-bisMGD cofactor/active site and the rate of intercenter electron transfer within NarGHI. (ii) The second phase is dependent on exhaustion of reducing substrate and dissociation of HOQNO from the Q_P site located in the vicinity of heme b_L. Thus, the inhibition of enzyme turnover observed in previous studies (*22*, *26*) arises primarily from inhibition of heme b_L oxidation rather than from inhibition of heme b_L reduction. Further characterization of HOQNO- and stigmatellin-dependent inhibition of NarGHI will require the use of stopped-flow kinetics to determine the extent of inhibition of heme reduction.

It has been suggested that electron transfer from quinol to nitrate can proceed along two pathways through the [Fe-S] clusters of NarH, one of which being sensitive to the absence of the highest potential [4Fe-4S] cluster (*6*, *25*). For this reason, we determined the effect of the absence of hemes b_H and b_L on the redox chemistry of the highest potential [4Fe-4S] cluster. No significant effect was observed compared to the effect of the absence of heme b_H on the E_m of the [3Fe-4S] cluster (Table 1). On this basis, it is unlikely that the highest potential [4Fe-4S] cluster is in close juxtaposition to heme b_H. In fact, two sets of evidence suggest that it is more likely located in a position relatively close to the Mo-bisMGD of NarG (but within NarH): (i) in apo-molybdo-NarGHI, there is a significant decrease in its E_m compared to its value in the cofactor-containing enzyme (*3*); and (ii) oxidation of the remaining [Fe-S] clusters is inhibited in a mutant lacking the highest potential [4Fe-4S] cluster (*49*).

Overall, we have demonstrated a significant structural link between the [3Fe-4S] cluster of NarH and heme b_H of NarI. The absence of the latter center in two mutants lacking the latter prosthetic group (NarGHI^{H56R} and NarGHI^{H205Y}) lowers the midpoint potential of the former prosthetic group and significantly modifies its EPR line shape. These results support the hypothesis that the two centers are in close juxtaposition within the holoenzyme, as is observed for the heme b_P and [3Fe-4S] cluster in the structure *W. succinogenes* fumarate reductase (*17*). In agreement with this, we have demonstrated that only heme b_L experiences a significant effect of pH on its E_m, suggesting that heme b_H and the [3Fe-4S] cluster are in a solvent-inaccessible location within the holoenzyme, located close to the NarH−NarI interface. The E_m values of both hemes appear to have a similar, significant dependence on pH in NarI(ΔGH), suggesting that the absence of NarGH exposes heme b_H to the aqueous milieu, in agreement with our earlier findings (*10*). The apparent solvent inaccessibility of heme b_H in the holoenzyme, the observation that inhibitors such as HOQNO and stigmatellin only affect the EPR line shape of heme b_L (*10*, *22*), and the detection of a single HOQNO binding site support a model for quinol binding and oxidation at a single site close to heme b_L.

REFERENCES

1. Blasco, F., Iobbi, C., Giordano, G., Chippaux, M., and Bonnefoy, V. (1989) *Mol. Gen. Genet. 218*, 249−256.
2. Richardson, D. J., and Watmough, N. J. (1999) *Curr. Opin. Chem. Biol. 3*, 207−219.
3. Rothery, R. A., Magalon, A., Giordano, G., Guigliarelli, B., Blasco, F., and Weiner, J. H. (1998) *J. Biol. Chem. 273*, 7462−7469.
4. Magalon, A., Asso, M., Guigliarelli, B., Rothery, R. A., Bertrand, P., Giordano, G., and Blasco, F. (1998) *Biochemistry 37*, 7363−7370.
5. Magalon, A., Lemesle-Meunier, D., Rothery, R. A., Frixon, C., Weiner, J. H., and Blasco, F. (1997) *J. Biol. Chem. 272*, 25652−25658.
6. Guigliarelli, B., Magalon, A., Asso, M., Bertrand, P., Frixon, C., Giordano, G., and Blasco, F. (1996) *Biochemistry 35*, 4828−4836.
7. Guigliarelli, B., Asso, M., More, C., Augier, V., Blasco, F., Pommier, J., Giordano, G., and Bertrand, P. (1992) *Eur. J. Biochem. 207*, 61−68.
8. Augier, V., Guigliarelli, B., Asso, M., Bertrand, P., Frixon, C., Giordano, G., Chippaux, M., and Blasco, F. (1993) *Biochemistry 32*, 2013−2023.
9. Augier, V., Asso, M., Guigliarelli, B., More, C., Bertrand, P., Santini, C., Blasco, F., Chippaux, M., and Giordano, G. (1993) *Biochemistry 32*, 5099−5108.
10. Rothery, R. A., Blasco, F., Magalon, A., Asso, M., and Weiner, J. H. (1999) *Biochemistry 38*, 12747−12757.
11. Berks, B. C., Page, M. D., Richardson, D. J., Reilly, A., Cavill, A., Outen, F., and Ferguson, S. J. (1995) *Mol. Microbiol. 15*, 319−331.
12. Walker, F. A., Huynh, B. H., Scheidt, W. R., and Osvath, S. R. (1986) *J. Am. Chem. Soc. 108*, 5288−5296.
13. Dou, Y., Admiraal, S. J., Ikeda-Saito, M., Krzywda, S., Wilkinson, A. J., Li, T., Olson, J. S., Prince, R. C., Pickering, I. J., and George, G. N. (1995) *J. Biol. Chem. 270*, 15993−16001.
14. Magalon, A. (1997) Ph.D. Thesis, Faculte des Sciences de Luminy, pp 86−90, Université de la Méditerranée, Marseille.
15. Hägerhäll, C., and Herderstedt, L. (1996) *FEBS Lett. 389*, 25−31.
16. Hägerhäll, C. (1997) *Biochim. Biophys. Acta 1320*, 107−141.
17. Lancaster, C. R. D., Kröger, A., Auer, M., and Michel, H. (1999) *Nature 402*, 377−385.
18. Ugulava, N. B., and Crofts, A. R. (1998) *FEBS Lett. 440*, 409−413.
19. Brandt, U., and Okun, J. G. (1997) *Biochemistry 36*, 11234−11240.
20. Magliozzo, R. S., McIntosh, B. A., and Sweeney, W. V. (1982) *J. Biol. Chem. 257*, 3506−3509.
21. Mayhew, S. G. (1999) *Eur. J. Biochem. 265*, 698−702.
22. Magalon, A., Rothery, R. A., Lemesle-Meunier, D., Frixon, C., Weiner, J. H., and Blasco, F. (1998) *J. Biol. Chem. 273*, 10851−10856.
23. Jones, W. R., Lamont, A., and Garland, P. B. (1980) *Biochem. J. 190*, 79−94.
24. Brito, F., DeMoss, J. A., and Dubourdieu, M. (1995) *J. Bacteriol. 177*, 3728−3735.
25. Giordani, R., Buc, J., Cornish-Bowden, A., and Cárdenas, M. L. (1997) *Eur. J. Biochem. 250*, 567−577.
26. Morpeth, F. F., and Boxer, D. H. (1985) *Biochemistry 24*, 40−46.

27. Rothery, R. A., Chatterjee, I., Kiema, G., McDermott, M. T., and Weiner, J. H. (1998) *Biochem. J. 332*, 35−41.
28. Blasco, F., Nunzi, F., Pommier, J., Brasseur, R., Chippaux, M., and Giordano, G. (1992) *Mol. Microbiol. 6*, 209−219.
29. Sambrook, J., Fritsch, E. F., and Maniatis, T. (1989) *Molecular Cloning: A Laboratory Manual*, 2nd ed., Cold Spring Harbor Laboratory Press, Cold Spring Harbor, NY.
30. Rothery, R. A., and Weiner, J. H. (1991) *Biochemistry 30*, 8296−8305.
31. Rothery, R. A., and Weiner, J. H. (1996) *Biochemistry 35*, 3247−3257.
32. Paulsen, K. E., Stankovich, M. T., and Orville, A. M. (1993) *Methods Enzymol. 227*, 396−411.
33. Cecchini, G., Ackrell, B. A. C., Deshler, J. O., and Gunsalus, R. P. (1986) *J. Biol. Chem. 261*, 1808−1814.
34. Okun, J. G., Lümmen, P., and Brandt, U. (1999) *J. Biol. Chem. 274*, 2626−2630.
35. Markwell, M. A. D., Haas, S. M., Bieber, L. L., and Tolbert, N. E. (1978) *Anal. Biochem. 87*, 206−210.
36. Lancaster, C. R. D., Gross, R., Haas, A., Ritter, M., Mäntele, W., and Simon, J. (2000) *Proc. Natl. Acad. Sci. U.S.A. 97*, 13051−13056.
37. Matsson, M., Tolstoy, D., Aasa, R., and Hederstedt, L. (2000) *Biochemistry 39*, 8617−8624.
38. Iverson, T. M., Luna-Chavez, C., Cecchini, G., and Rees, D. C. (1999) *Science 284*, 1961−1966.
39. Rothery, R. A., and Weiner, J. H. (1998) *Eur. J. Biochem. 254*, 588−595.
40. Hägerhäll, C., Magnitsky, S., Sled, V. D., Schröder, I., Gunsalus, R. P., Cecchini, G., and Ohnishi, T. (1999) *J. Biol. Chem. 274*, 26157−26164.
41. Ingledew, W. J., Ohnishi, T., and Salerno, J. C. (1995) *Eur. J. Biochem. 227*, 903−908.
42. Sato-Watanabe, M., Mogi, T., Ogura, T., Kitagawa, T., Myoshi, H., Iwamura, H., and Anraku, Y. (1994) *J. Biol. Chem. 269*, 28908−28912.
43. Sato-Watanabe, M., Itoh, S., Mogi, T., Matsuura, K., Miyoshi, H., and Anraku, Y. (1995) *FEBS Lett. 374*, 265−269.
44. Ermler, U., Michel, H., and Schiffer, M. (1994) *J. Bioenerg. Biomembr. 26*, 5−15.
45. Allen, J. P., and Williams, J. C. (1998) *FEBS Lett. 438*, 5−9.
46. Zhang, Z., Huang, L., Shulmeister, V., Chi, Y., Kim, K. K., Hung, L., Crofts, A. R., Berry, E. A., and Kim, S. (1998) *Nature 392*, 677−684.
47. Bayman, F., Robertson, D. E., Dutton, P. L., and Mäntele, W. (1999) *Biochemistry 38*, 13188−13199.
48. Guergova-Kuras, M., Kuras, R., Ugulova, N., Hadad, I., and Crofts, A. R. (2000) *Biochemistry 39*, 7436−7444.
49. Magalon, A., Rothery, R. A., Giordano, G., Blasco, F., and Weiner, J. H. (1997) *J. Bacteriol. 179*, 5037−5045.

BI002393K